Radiation from Flare-Accelerated Particles Impacting the Sun

Gerald H. Share and Ronald J. Murphy
E.O. Hulburt Center for Space Research, Naval Research Laboratory Washington, DC 20375

Short title: RADIATION FROM FLARE-ACCELERATED PARTICLES IMPACTING THE SUN

Abstract. We discuss how remote observations of gamma-ray lines and continuum provide information on the population of electrons and ions that are accelerated at the flare site. The radiation from these interactions also provides information on the composition of the flaring atmosphere. We focus our discussion on recent *RHESSI* observations and archival observations made by *SMM* and *Yohkoh*.

1. INTRODUCTION

Eruptive solar events such as flares and coronal mass ejections (CME's) accelerate electrons and ions to high energies. The solar energetic particles (SEP) that reach interplanetary space have origins in both flares and CME's (e.g. Reames 1999) and there is debate over their relative importance (e.g. Cane et al. 2003; Tylka et al. 2005; Li and Zank 2005). Timing (e.g. Tylka et al. 2003) and composition studies support the idea that flares are primarily responsible for the 'impulsive' electron and ^{3}He-rich particle events in space and also contribute the seed population (Mason, Mazur, and Dwyer 1999) for 'gradual' events that have their origin in CME produced shocks. The processes that impulsively accelerate particles into interplanetary space along open magnetic field lines may also generate the ions and electrons along closed loops that impact the solar atmosphere and photosphere.

In Figure 1 we show a simplified model depicting injection of accelerated particles (e.g. Miller et al. 1997; Aschwanden 2004) onto a closed magnetic loop, their transport, and their impact on the solar atmosphere. The resulting continuum and line γ radiation provides the means to remotely measure the characteristics of these trapped particles and relate them to flare-produced particles that escape from the Sun on open field lines. The flares of 2003 October 28 and November 2, and 2005 January 20 offer the best opportunity for making simultaneous measurements of these two particle populations. Other papers in this monograph will discuss the particles measured in space. In this paper we discuss the relationship between the >100 keV photon emissions and both the accelerated particles and the solar material which they impact. We summarize some preliminary results derived from these new *RHESSI* and archival *SMM* and *Yohkoh* observations.

2. WHAT PRODUCTS OF PARTICLE INTERACTIONS TELL US ABOUT FLARE-ACCELERATED IONS

In this Section we briefly discuss the products of flare-accelerated electrons and ions that impact the Sun (Figure 1). Relativistic electrons produce bremsstrahlung continuum that reflects their spectrum. For example an electron spectrum following a power-law in energy with index β produces a photon spectrum with index $\sim \beta - 1$(Ramaty et al. 1993). Protons and α-particles interact with ambient solar nuclei to produce neutrons, γ-ray lines from transitions of excited nuclei to lower-energy states, and positrons from radioactive nuclei (Ramaty, Kozlovsky, and Lingenfelter 1979). If the incident particles have energies above a few hundred MeV/nucleon π mesons are produced that decay with emission of electrons, positrons, and γ rays (Murphy, Dermer, and Ramaty 1987). The neutrons can escape from the Sun and be detected at Earth before they decay (e.g. Chupp et al. 1982), decay at the Sun, or be captured on H or ^{3}He; capture on H produces ^{2}H with emission of a 2.223-MeV γ-ray having a width of a few eV, while capture on ^{3}He produces no γ radiation. The γ-ray lines from excited nuclei are moderately broadened because the excited nuclei recoil from impact. Isotropic proton and α-particle impacts on ^{12}C produce $\sim$ 75 and 110 keV FWHM line widths. Much larger widths ($\sim$ 20% FWHM) result from interactions of accelerated heavy ions, e.g. ^{12}C, when they de-excite after interacting with ambient H or He. Positrons produced in the interactions annihilate with electrons to produce a line at 511 keV and a continuum below that energy.

In Figure 2 we plot the γ-ray spectrum observed from 200 keV to 8.5 MeV by *RHESSI* during the 2003 October 28 flare. The spectrum reveals all the different components described above. The most distinct features are the 511-keV annihilation line and 2.223-MeV neutron capture line that rise above both the electron bremsstrahlung continuum and 'narrow' and 'broad' nuclear lines from proton/α and heavy-ion interactions, respectively.

2.1. Bremsstrahlung from Flare-Accelerated Electrons

The best fitting bremsstrahlung continuum shown in Figure 2 has a shape approximated by two power laws with spectral indices ~ 3.8 and 2.1 below and above an ~ 460 keV break energy, respectively. This hardening is characteristic of many γ-ray flares (e.g. McTiernan and Petrosian 1991) and suggests that the accelerated electron spectra may harden near ~ 1 MeV. The hardening in the October 28 flare may, in part, be due to a separate electron component from decay of high-energy pions whose neutral component was detected in high-energy γ-rays by *CORONAS-F* (Kuznetsov et al. 2005). It will be interesting to compare the inferred electron spectrum at the Sun with that observed in space for this flare.

The bremsstrahlung spectrum hardened significantly with time during the flare. This hardening is reflected in the decreasing power-law indices above and below the break energy that we plot in Figure 3; there was a similar hardening during the November 2 flare. Is there any evidence for such a hardening of the electron spectrum observed in space? Other flares exhibit significantly different behavior as we illustrate in Figure 4 which displays variations in the single power law index fit to the bremsstrahlung spectrum from the 1989 March 6 flare observed by *SMM.*

2.2. Nuclear Lines from Accelerated Particle Interactions

The 2003 October 28 and November 2 and 2005 January 20 flares offer a unique opportunity to compare accelerated ion spectra and composition at the Sun and in interplanetary space. Other papers in this volume discuss SEP observations. We discuss preliminary observations of the characteristics of the accelerated particles at the Sun inferred from γ-ray observations.

2.2.1. Directionality of interacting protons and α-particles. The shapes of the 'narrow' nuclear lines provide information on the angular distribution of interacting protons and α-particles. We plot four of the lines used in the study of the 2003 October 28 flare in Figure 5. The lines are red-shifted from their laboratory energies (Smith et al. 2004; Gan 2005) by an amount that is consistent with both *INTEGRAL* observations (Gros et al. 2004) and what is calculated for a broad downward-directed distribution of accelerated particles as found in a study of 19 *SMM* flares (Share et al. 2002). We have simultaneously fit the energies of strong nuclear de-excitation lines in three *RHESSI* and 19 *SMM* flares to study their redshift as a function heliocentric angle. In Figure 6 we plot the % line shift for these 22 flares relative to the 4.439 MeV laboratory energy of the ^{12}C line. *RHESSI* detected larger redshifts than expected for the heliocentric angles of the 2002 July 23 (Smith et al. 2003) and 2003 November 2 flares (Murphy and Share 2005). We are currently studying whether the distribution of *SMM* redshifts is consistent with such large shifts. Such shifts suggest that the magnetic loops constraining the particles are tilted from the normal (Smith et al. 2003).

2.2.2. Spectrum of accelerated protons and α-particles. Line-flux ratios provide an estimate of the energy spectrum of accelerated protons and α-particles that impact the solar atmosphere (e.g. Murphy and Share 2005). This is possible because the cross sections for γ-ray line production can have significantly different energy dependences (Kozlovsky, Murphy, and Ramaty 2002). Comparison of fluxes in the ^{20}Ne (1.63 MeV) line and in the ^{16}O (6.13 MeV) and ^{12}C (4.43 MeV) lines provides information on the spectrum between ~ 2 and 20 MeV nucleon^{-1}. To determine the spectrum from $\sim 10-50$ MeV nucleon^{-1} (or hundreds of MeV nucleon^{-1} if pions are produced) we typically compare the 511-keV annihilation line with the ^{12}C and ^{16}O lines. Comparison of the neutron-capture line with the ^{12}C and ^{16}O lines provides information on the spectrum from $\sim 10-100$ MeV nucleon^{-1}.

Ramaty et al. (1995, 1996) evaluated the flare-averaged accelerated-particle spectra from 19 *SMM* flares (Share and Murphy 1995). This determination is dependent on both the assumed ambient and accelerated particle compositions. Assuming spectra following power laws the average index was ~ 4.3 between ~ 2 and 20 MeV nucleon^{-1} (Share et al. 2002; Murphy and Share 2005). From a preliminary analysis we find that the spectra of the 2003 October 28 and November 2 flares in the same energy range were considerably harder than this average; the power-law indices were measured to be 2.5 ± 0.4 and 2.5 ± 0.9, respectively (Share et al. 2004a). Gan (2005) suggested that a steeper spectrum would be derived for an ambient Ne/O concentration of 0.15 in lieu of the value of 0.25 that was assumed (Ramaty et al. 1996). Tatischeff, Kiener, and Gros (2005) also derived a steeper spectrum for the October 28 flare based on *INTEGRAL* observations of fluxes in the C and O de-excitation lines and suggested that the ambient abundances of these nuclei may differ from current solar models. We note, however, that a hard spectrum is required to produce the observed 511 keV line flux (Share et al. 2004a) and the π^o-decay γ-rays observed by *CORONAS-F* (Kuznetsov et al. 2005). It appears likely that solar γ-ray line observations will add to the growing debate about solar abundances (e.g. Antia and Basu 2005; Bahcall, et al. 2005; Drake and Testa 2005), some of which have been derived using SEP data.

Perhaps the hardest spectrum of accelerated particles ever observed to impact the Sun occurred during the 2005 January 20 flare. In Figure 7, we show a spectrum integrated over the entire impulsive phase of the January 20 flare. The spectrum is dominated by a hard bremsstrahlung continuum with strong 511-keV annihilation and 2.223-MeV neutron-capture line emission, and relatively weak nuclear de-excitation line emission. Based on the (511-keV)/(2.223-MeV) flux ratio for a flare at $\sim 60^\circ$ heliocentric angle, we estimate a power-law index of ~ 2.2 for solar impacting particles ≥ 50 MeV nucleon^{-1}. This is consistent with an index of 2.15 observed for SEP's (Mewaldt et al. 2005). For such a hard spectrum most of the 511 keV photons come from π^+-decay positrons. This is consistent with the observation of neutral pion-decay gamma rays by CORONAS-F (Priv. comm. V. Kurt, 2005).

2.2.3. Accelerated helium abundance. The intensity of the α-^{4}He fusion lines (^{7}Be and ^{7}Li) in flares observed by the *SMM* spectrometer has been found to be more intense than expected for assumed accelerated α/p and ambient ^{4}He/H abundances of 0.1 (Share and Murphy 1997). Kozlovsky, Murphy, and Share (2004) set a 1 σ lower limit of 0.35 to the α/p ratio in the 2002 July 23 flare observed by *RHESSI*, consistent with the *SMM* observations. Plotted in Figure 8 is the spectrum between 350 and 650 keV accumulated during the first 4 minutes of the 2003 October flare after subtracting bremsstrahlung and nuclear contributions. The dotted line shows the best fit to the α-^{4}He line shape for a downward isotropic distribution of accelerated particles. (In Section 4.2 we discuss the annihilation line and its continuum that are also shown in the Figure.) If we assume that the accelerated-particle power-law index is 2.5 and ambient ^{4}He/H = 0.1, we obtain preliminary accelerated α/p ratios of 0.65 (-0.3, + 0.15) and 0.4 (-0.15, +0.2) for the 2003 October 28 and November 2 *RHESSI* flares, respectively (Share et al. 2004b). Due to differences in the p and α cross sections, we derive lower α/p ratios for softer particle spectra. We note that if the protons and α-particles had different spectral indices this will affect the value of the accelerated α/p ratio derived from the gamma-ray line measurements (Toner and Mackinnon 2004). Gan (2005) concluded that the α/p ratio in both flares probably did not exceed 0.1. He based his conclusion on comparative studies of the Ne/O and n-capture/C line flux ratios; this method is rather indirect because the results are also dependent on other factors. Tatischeff et al. (2005) used a similar method but did not attempt to draw any conclusions about the ratio. As we mentioned earlier it is possible to use the measured de-excitation line shape to estimate the α/p ratio (Smith et al. 2003). This method is most sensitive to the ratio for softer accelerated particle spectra than observed in these two flares, however.

Our estimate of the accelerated α/p ratio is inversely dependent on the ambient ^{4}He/H ratio, assumed to be 0.1. Feldman and Landi (2005) recently measured a ^{4}He/H ratio of 0.122 ± 0.024 in high-temperature solar flare plasmas. Mandzhavidze, Ramaty, and Kozlovsky (1997) suggested a method to determine whether these high α-He line fluxes are due to an elevated α/p ratio and/or to an elevated ambient ^{4}He/H ratio This requires comparison of the fluxes in lines produced by α-^{56}Fe (339 keV) and p-^{56}Fe (847 keV) reactions. There is evidence for a weak line at 339 keV in data obtained with moderate resolution NaI spectrometers, consistent with an elevated α/p ratio (Share and Murphy 1998). Our preliminary assessment is that the spectra of the October 28 and November 2 flares may be too hard for the 339-keV line to be detected because its production cross section peaks at low energies.

The key line features for understanding the ^{3}He abundance appear near 0.937, 1.040, and 1.08 MeV (Mandzhavidze et al. 1997). Share and Murphy (1998) found evidence for an average ^{3}He/^{4}He ratio of 0.1 in flares observed by *SMM* and Mandzhavidze et al. (1999) additionally suggested that a ratio as high as 1 could occur in some flares. Such high ^{3}He/^{4}He ratios are consistent with what is observed in some solar energetic particle events. Mason et al. (2002) report ratios for 14 impulsive particle events that varied between $\sim$ 0.1 and 6.5. *RHESSI* can more easily resolve the ^{3}He lines from other nearby lines. Based only on the 937-keV line, we obtained preliminary 99% upper limits of 0.8 and 2.5 on the ^{3}He/^{4}He ratios in the October 28 and November 2 flares, respectively (Share et al. 2004b).

2.2.4. Accelerated heavy ions. From the fit to the overall *RHESSI* spectrum shown in Figure 2, we note that the broad nuclear lines (solid curve) that are in part due to accelerated heavy ions impacting on ambient H can contribute up to about 25% of the total flux in certain energy ranges. We see evidence for the broad lines near 4 MeV and 6 MeV, attributable to flare-accelerated ^{12}C and ^{16}O. Unfortunately, there is an intense continuum below the 2.223-MeV line that may mask the presence of the broadened lines at lower energy, including the ^{56}Fe line near 847 keV observed in flares by *SMM*. Share and Murphy (1999) presented the broad-line spectrum from the sum of 19 flares observed by *SMM*; this spectrum is plotted in Figure 9 after the narrow lines and bremsstrahlung have been subtracted. Highly Doppler-broadened lines from accelerated ^{56}Fe, ^{12}C, and ^{16}O appear to be resolved. Analysis indicated an $\sim 5\times$ excess in the abundance of accelerated ^{56}Fe relative to its ambient abundance, similar to that found in SEPs. The shape of the spectrum is also in agreement with calculations (solid curve) for accelerated particles with an impulsive SEP composition, α/p = 0.5, power-law index 4.5, and downward isotropic distribution. Thus impulsively accelerated particles at the Sun and in space may have similar compositions. We have preliminary evidence that the accelerated Fe concentration may be highly variable in flares. In Figure 10 we plot the broad ^{56}Fe line flux vs. the broad ^{12}C line flux observed in 19 *SMM* flares. We note that some of the variability may be due to flare-to-flare variations in the spectra of the accelerated particles.

Chadwick et al. (1999) have performed detailed calculations of the total γ-ray yield for various nuclei that can be used to determine the shape of the unresolved nuclear-line and continuum spectrum from excited nuclei that have compromised our ability to study the accelerated heavy-ion component in flares. The histogram plotted in Figure 9 is a preliminary estimate of the shape of the unresolved nuclear line and continuum emitted from ^{28}Si.

3. COMPARISON OF ACCELERATED ELECTRONS AND IONS

3.1. Temporal Variations in Accelerated Ions and Electrons

Important information about the acceleration and transport of electrons and ions can be obtained by a comparison of the time histories observed in different energy bands of the hard X-ray and γ-ray spectra. Chupp (1990) discussed an early study of *SMM* data indicating that the peaks in individual bursts observed in the 4.1 - 6.4 MeV energy band (mostly due to ion interactions) were delayed between 2 s and 45 s from the corresponding maxima observed in the electron bremsstrahlung continuum near 300 keV (see also Share and Murphy 2004c). This delay appears to be proportional to the rise time of the pulse. Some of these delays may be explained by transport effects in magnetic loops (e.g. Murphy and Share 2005).

Such delay analyses may not reveal the true complexity of the variation between the nuclear and electron emissions, however. In Figure 11 we show variations in the nuclear-line to bremsstrahlung ratio with time in two flares observed by *Yohkoh* (in the 4-7 MeV region) and one observed by SMM (from 0.3-8.5 MeV). The nuclear/bremsstrahlung ratio appears to increase with time during 2001 August 25 flare, decrease with time during the 2001 April 15 flare, and show variable behavior in the 1989 March 6 flare.

3.2. Energy in Accelerated Electrons and Ions

Using the derived accelerated spectra it is possible to compare the energies contained in flare accelerated ions and electrons. Ramaty and Mandzhavidze (2000) performed this study for 19 flares observed by *SMM* and found that the ions and electrons contained comparable energies. Emslie et al. (2004) obtained a similar result for the 2002 July 23 flare; for the 2002 April 21 flare they placed an upper limit on the energy in ions that is just above that measured in electrons. We have made a preliminary estimate of the energies contained in protons in the 2003 October 28 and November 2 flares. We use both *RHESSI* and *INTEGRAL* (Gros et al. 2004) data for the October 28 flare. The energy in protons is strongly dependent on the both the spectrum and low-energy cutoff energy. The γ-ray line studies provide information on protons with energies $\gtrsim$ 3 MeV. We can obtain an upper limit on the energy contained in the protons by assuming that the spectrum extends without a break down to 0.1

MeV. For a power-law index of 3 we estimate that protons contained $\sim 1.5 \times 10^{32}$ ergs in the October 28 flare and $\sim 0.5 \times 10^{32}$ ergs in the November 2 flare. At present there are no estimates for the energy content in electrons for these flares.

4. ACCELERATED PARTICLES PROBE THE SOLAR ATMOSPHERE AND PHOTOSPHERE

Flare-accelerated protons and α-particles and secondary positrons act as probes of the flaring chromosphere and photosphere. Gamma-ray emission from their interactions have revealed a dynamic chromosphere that exhibits the FIP effect seen in the corona and puzzling evidence for striking temperature and ionization changes.

4.1. FIP Effect at Chromospheric Densities

Fluxes of narrow lines from ambient heavy nuclei observed from 19 flares (Share and Murphy 1995) have been used by Ramaty et al. (1995)) to infer that there is a strong FIP effect where the particles interact ($\gtrsim 10^{14}$ H cm^{-3}; see e.g. Murphy and Share 2005), suggesting that the ambient plasma has a coronal composition. Laming (2004) provided an explanation for the FIP effect under less dynamic conditions at lower densities ($\sim 10^{12}$H cm^{-3}). Share and Murphy (1995) pointed out that the FIP ratio appears to vary from flare-to-flare. The average low-FIP (Fe, Mg, Si) to high-FIP (Ne, C, O) line ratio for 19 *SMM* flares was ~ 0.45. Murphy et al. (1997) showed evidence that the FIP ratio can increase with time in an extended flare observed by *CGRO*/OSSE. Similar temporal variation has been observed by *SMM* and *RHESSI*. For example, in Figure 12 we show a plot of the time variation of the low FIP/high FIP line ratio in the 1989 March 6 flare observed by *SMM* suggestive of an increase with time. More convincing evidence for increase in the ratio is provided by *RHESSI* observations of the 2003 October 28 and November 2 flares (Share et al. 2004b; Shih et al. 2004) plotted in Figure 13. These observations suggest that the accelerated particles interact in ambient compositions that change with time. It would be of interest to determine whether chromospheric evaporation of this fractionated material could contribute significantly to the coronal material and provide seed material for subsequent acceleration into interplanetary space.

4.2. Positrons Probe the Chromosphere and Photosphere

Positrons are emitted in the radioactive decay of nuclei produced when flare-accelerated ions interact with the solar atmosphere (Kozlovsky, Lingenfelter, and Ramaty 1987). The positrons annihilate directly and through formation of positronium. Annihilation yields either a line (2 photons) or continuum (3 photons) depending on the conditions of the ambient medium (Crannell et al. 1976). Until the *RHESSI* 2002 July 23 flare observation (Share et al. 2003), the 511-keV line had not been clearly resolved. The line had a width of 8.1 ± 1.1 keV which was consistent with both annihilation in an ionized medium $4 - 7 \times 10^5$ K and in a quiet atmosphere at 6000K. The latter location, however, does not provide enough column depth for the production of radioactive nuclei and for the slowing down and annihilation of the positrons.

We have now studied annihilation radiation in four *RHESSI* flares. The 2003 October 28 flare produced the largest fluence of annihilation radiation observed to date (Share et al. 2004a). It also displayed a remarkable change in width of the 511-keV line (see bottom panel of Figure 14). The width of the line changed from an average of $\sim$6.5 keV to $\sim$1 keV within about two minutes when there was no marked change in the fluxes observed. This difference is most clearly shown in Figure 15. There was a rapid change in the relative flux in the measured continuum below the line early in the flare (see third panel in Figure 14). This step-function increase below the line can be seen in Figure 8. We believe that the high continuum flux in the first 2-3 minutes is due to Compton scattering of the annihilation line under 5 to 10 g cm^{-2} of H. This depth is consistent with an e^+-origin from decay of π^+-mesons; γ- rays from π^o-meson decay were observed a few minutes earlier by *CORONAS-F* (Kuznetsov et al. 2005). From fits to the line shapes we conclude that the broad line is likely to be due to annihilation in a $> 2 \times 10^5$ K medium and that the narrow line is produced at temperatures $< 10^4$ K, albeit in a highly ionized medium. These observations raise issues concerning the character of the flaring atmosphere.

There have been two new developments since publication of the 2003 October 28 and November 2 annihilation radiation studies. Murphy et al. (2005) have developed an improved algorithm that calculates the 511-keV annihilation line spectrum and relative strength of the 3-γ continuum for a wide range of physical environments relevant to the flaring solar atmosphere. We are using these calculations to study the annihilation emission from all the flares observed by *RHESSI*. Recent studies indicate that the annihilation line shape is consistent with Gaussians over the entire October 28 flare, implying temperatures $> 2 \times 10^5$ K during the first 10 min and $< 10^4$ K (>20% ionized) during the last 10 min. During both intervals, the inferred density is significantly $> 10^{14}$ H cm^{-3}. What is especially puzzling is the rapid, 2 minute, transition from broad to narrow line width (Figures 14 & 15). There is some evidence that this transition occurs as the flare ribbon moved over the umbra of the sunspot (Priv. comm. C. Schrijver 2005). The line observed during the November 2 flare is also broad but it can be fit with the shape expected for annihilation in a quiet solar atmosphere at a temperature of 5000 K (Murphy et al. 2005); there is uncertainty whether the continuum below the line is consistent with this origin, however.

The annihilation line studies, the hardness of the accelerated particle spectra, and detection of pion-decay radiation suggest that we are also studying sub-photospheric conditions with gamma rays. It is puzzling how the apparently high temperatures and ionization states can be supported at these densities. A new aspect is the detection of acoustic waves below the photosphere following the October 28 and 29 flares (Donea and Lindsey 2005). Our preliminary estimates indicate that there is sufficient energy in $\gtrsim$ 100 MeV protons to account for the acoustic waves. If this association with high-energy protons is correct, acoustic waves should have been detected after the 2005 January 20 flare. The intense hard bremsstrahlung and weak de-excitation line emission in the January 20 flare resembles the electron-rich events suggested by Rieger et al. (1998). Could these be due to episodes with very hard proton spectra that produce pions? The hard bremsstrahlung then could result from pion-decay electrons and positrons.

4.3. Search for Photospheric ^{3}He using Fast Neutrons

Neutrons produced in accelerated particle interactions with the solar atmosphere can escape the Sun, decay, or slow down and get captured by either H or ^{3}He. Capture on H produces a line at 2.223 MeV while capture on ^{3}He is radiationless. Both the angular distribution of accelerated particles and concentration of ^{3}He affect the time profile of the capture line. Murphy et al. (2003) have compared the time history of the line with calculations to determine both the angular distribution of accelerated particles and photospheric ^{3}He concentration in the 2002 July 23 flare. The nuclear-line flux has been used as a surrogate for the acceleration time profile. A physically based transport model has been used in performing the analysis. We find that the accelerated particles suffer significant pitch-angle scattering in the corona, yielding a broad downward-directed distribution. Because pitch-angle scattering, spectral hardness, and ^{3}He all affect the neutron-capture line time history and the nuclear line flux was relatively weak, the photospheric ^{3}He abundance is not well constrained (^{3}He/H = (0.5 - 10.0) $\times 10^{-5}$). Tatischeff, Kiener, and Gros (2005)) obtained a similar result for the 2003 October 28 flare.

Acknowledgments. We wish to thank David Smith, Albert Shih, Bob Lin, Richard Schwartz, Kim Tolbert, and the rest of the *RHESSI* team for the excellent performance of the instrument, its calibration, and for the analysis routines that have made this work possible.

This work was supported by NASA DPR 10049 and NNG04ED181, and by the Office of Naval Research.

References

Antia, H. M., and S. Basu, The discrepancy between solar abundances and helioseismology, *Astrophys. J., 620,* L129-L132, 2005.

Aschwanden, M., *Physics of the Solar Corona, An Introduction,* 842 pp., Springer/Praxis Publishing, Chichester, UK, 2004.

Bahcall, J. N., and S. Basu, Helioseismological implications of recent solar abundance determinations, *Astrophys. J., 618,* 1049-1056, 2005.

Cane, H. V., T. T. von Rosenvinge, C. M. S. Cohen, and R. A. Mewaldt, Two components in major solar particle events, *Geophys. Res. Lett., 30*, 8017, doi:10.1029/2002GL016580, 2003.

Chadwick, M. B., P. G. Young, S. Chiba, S. C. Frankle, et al., Cross-section evaluations to 150 MeV for accelerator-driven systems and implementation in MCNPX, *Nucl. Sci. & Eng.131,*, 293-328, 1999.

Chupp, E.L., Transient particle-acceleration associated with solar flares, *Science 250*, 229-236, 1990.

Chupp, E. L., D. J. Forrest, J. M. Ryan, J. Heslin, C. Reppin, K. Pinkau, G. Kanbach, E. Rieger, and G. H. Share, A direct observation of solar neutrons following the 0118-UT flare on 1980 June 21, *Astrophys. J., 263,*, L95-L99, 1982.

Crannell, C. J., and G. Joyce, R. Ramaty, and C. Werntz, Formation of 0.511 MeV line in solar flares, *Astrophys. J., 210,* 582-592, 1976.

Donea, A.-C., and C. Lindsey, Seismic emission from the solar flares of 2003 October 28 and 29, *Astrophys. J., 000,* 000-000, 2005.

Drake, J. D., and Testa, P., The abundance of neon in the local cosmos and the solar model problem, *Astrophys. J., 000,* 00-00, 2005.

Emslie, A.G., et al., Energy Partition in Two Solar Flare/CME Events, *J. Geophys. Res., 109*, A10104, 2004.

Feldman, U., and E. Landi, Helium abundance in high-temperature solar flare plasmas, *Astrophys. J., 619,* 1142-1152, 2005.

Gan, W. Q., Gamma-ray line analysis for the flares of 28 October and 2 November 2003, *Adv. Sp. Res.*in print, 2005.

Gros, M., V. Tatischeff, J. Kiener, B. Cordier, G. Weidenspointer, et al., *INTEGRAL*/SPI observation of the 2003 Oct 28 solar flare, *Proc.* 5^{th} *INTEGRAL Workshop, Munich, Germany*, *ESA SP-552*, 669-676, 2004.

Kozlovsky, B., R. E. Lingenfelter, and R. Ramaty, Positrons from accelerated particle interactions, *Astrophys. J., 316,* 801-818, 1987.

Kozlovsky, B., R. J. Murphy, and R. Ramaty, Nuclear deexcitation gamma-ray lines from accelerated particle interactions, *Astrophys. J. (Supp.), 141,* 523-541, 2002.

Kozlovsky, B., R. J. Murphy, and G. H. Share, Positron-emitter production in solar flares from ^{3}He reactions, *Astrophys. J., 604,* 892-899, 2004.

Kuznetsov, S. N., V. G. Kurt, B. Y. Yushkov, I. N. Myagkova, and K. Kudela, Gamma-ray and high-energy particle measurements of the solar flare of 28 October 2003 on board *CORONAS-F*, *Sol. Phys. –,* 0-0, 2005.

Laming, J. M., A unified picture of the first ionization potential and inverse first ionization potential effects, *Astrophys. J., 614,* 1063-1072, 2004.

Li, G., and G. P. Zank, Mixed particle acceleration at CME-driven shock and flares, *Geophys. Res. Lett., 32,* L02101, doi:10.1029/2004GL021250, 2005.

Mandzhavidze, N., R. Ramaty, and B. Kozlovsky, Solar atmospheric and solar flare accelerated helium abundances and gamma-ray spectroscopy, *Astrophys. J., 489,* L99-L102, 1997.

Mandzhavidze, N., R. Ramaty, and B. Kozlovsky, Determination of subcoronal ^{4}He and solar flare-accelerated ^{3}He and ^{4}He from gamma-ray spectroscopy, *Astrophys. J., 518,* 918-925, 1999.

Mason, G. M., J. E. Mazur, and J. R. Dwyer, ^{3}He enhancements in large solar energetic particle events, *Astrophys. J., 525,* L133-L136, 1999.

Mason, G. M., M. E. Wiedenbeck, J. A. Miller, et al., Spectral properties of He and heavy ions in ^{3}He-rich solar flares, *Astrophys. J., 574,* 1039-1058, 2002.

Masuda, S, T. Kosugi, H. Hara, and Y. Ogawara, A loop top hard x-ray source in a compact solar-flareas evidence for magnetic reconnection, *Nature 371,* 495-497, 1994.

McTiernan, J. M., and V. Petrosian, Center-to-limb variations of characteristics of solar flare hard x-ray and gamma-ray emission, *Astrophys. J., 379,* 381-39, 1991.

Mewaldt, R., C. Cohen, A. Labador, M. Looper, and G. Mason, Space Weather Aspects of the January 20, 2005 Solar Energetic Particle Event, *ACE News no. 87 - Feb 23, 2005,* Calif. Inst. of Tech., Pasadena, CA, 2005.

Miller, J. A., P. J. Cargill, A. G. Emslie, G. D. Holman, B. R. Dennis, T. N. LaRosa, R. M. Winglee, S. G. Benka, and Tsuneta, S., Critical issues for understanding particle acceleration in impulsive flares, *J. Geophys. Res., 102,*14631-14659, 1997.

Murphy, R. J., C. D. Dermer, and R. Ramaty, High-energy processes in solar flares, *Astrophys. J. (Supp.), 63,* 721-748, 1987.

Murphy, R. J., B. Kozlovsky, J. G. Skibo, and G. H. Share, The Physics of Positron Annihilation in the Solar Atmosphere, *Astrophys. J.,* , 000-000, 2005.

Murphy, R. J., and G. H. Share, What gamma-ray de-excitation lines reveal about solar flares, *Adv. Sp. Res.*in print, 2005.

Murphy, R. J., G. H. Share, J. E. Grove, W. N. Johnson, R. L. Kinzer, M. S. Strickman, and G. V. Jung, Accelerated particle composition and energetics and ambient abundances from gamma-ray spectroscopy of the 1991 June 4 solar flare, *Astrophys. J., 490,*, 883-900, 1997.

Murphy, R. J., G. H. Share, X.-M. Hua, R. P. Lin, D. M. Smith, and R. A. Schwartz, Physical implications of *RHESSI* neutron-capture line measurements, *Astrophys. J., 595,*, L93-L97, 2003.

Ramaty, R., B. Kozlovsky, and R. E., Lingenfelter, Nuclear gamma-rays from energetic particle interactions, *Astrophys. J. (Supp.), 40,* 487-526, 1979.

Ramaty, R. and N. Mandhavidze, Highly energetic physical processes and mechanisms for emission from astrophysical plasmas, *IAU Symposia 195*, 123-132, 2000.

Ramaty, R., N. Mandzhavidze, B. Kozlovsky, and J. G. Skibo, Acceleration in solar flares – interacting particles versus interplanetary particles, *Adv. Sp. Sci 19 (9),* 275-284, 1993.

Ramaty, R., N. Mandzhavidze, B. Kozlovsky, and R. J. Murphy, Solar atmospheric abundances and energy content in flare-accelerated ions from gamma-ray spectroscopy, *Astrophys.*

J., 455, L193-L196, 1995.

Ramaty, R., N. Mandzhavidze, and B. Kozlovsky, Solar atmospheric abundances from gamma ray spectroscopy, *High Energy Solar Physics, ed. R. Ramaty, N. Mandzhavidze, and X-M Hua, AIP Conf. Proc., 374* 172-183, 1996.

Reames, D. V., Particle acceleration at the Sun and in the heliosphere, *Space Sci. Rev. 90,* 413-491, 1999.

Rieger, E., W. Q. Gan, and H. Marschhäuser, Gamma-ray line versus continuum emission of electron-dominated episodes during solar flares, *Solar Physics 183,* 123-132, 1998.

Share, G. H., and R. J. Murphy, Gamma-ray measurements of flare-to-flare variations in ambient solar abundances, *Astrophys. J., 452,* 933-943, 1995.

Share, G. H., and R. J. Murphy, Intensity and directionality of flare-accelerated alpha-particles at the Sun, *Astrophys. J., 485,* 409-418, 1997.

Share, G. H., and R. J. Murphy, Accelerated and ambient He abundances from gamma-ray line measurements of flares, *Astrophys. J., 508,* 876-884, 1998.

Share, G. H., and R. J. Murphy, Gamma-ray measurement of energetic heavy ions at the sun, *Proc. of the 26th Cosmic Ray Conference, 6,* 13-16, 1999.

Share, G. H., and R. J. Murphy, Solar Gamma-Ray Line Spectroscopy Physics of a Flaring Star, in Stars as Suns: Activity, *Evolution and Planets, IAU Conf. Series 219*, ed. A.K. Dupree and A.O. Benz, 133-144, 2004c.

Share, G. H., R. J. Murphy, J. Kiener, and N. de Sereville, Directionality of solar flare accelerated protons and alpha particles from gamma-ray line measurements, *Astrophys. J., 573,* 464-470, 2002.

Share, G. H., R. J. Murphy, J. G. Skibo, D. M. Smith, H. S. Hudson, R. P. Lin, A. Y. Shih, B. R. Dennis, and R. A. Schwartz, High-resolution observation of the solar positron-electron annihilation line, *Astrophys. J., 595,* L85-L88, 2003.

Share, G. H., R. J. Murphy, D. M. Smith, R. A. Schwartz, and R. P. Lin, *RHESSI* e^+ - e^- annihilation radiation observations: implications for conditions in the flaring solar chromosphere, *Astrophys. J., 615,* L169-L172, 2004a.

Share, G. H., R. J. Murphy, D. M. Smith, R. P. Lin, and A. Y. Shih, Accelerated particle spectra and abundances in the 2003 October 28 and November 2 solar flares (abstract), *Fall AGU Mtg.*, SH13A-1135, 2004b.

Shih, A. Y., D. M. Smith, R. P. Lin, G. H. Share, R. J. Murphy, and R. A. Schwartz, *RHESSI* observations of gamma-ray lines from solar flares (abstract), *Fall AGU Mtg.*, SH24A-01, 2004.

Smith, D. M., G. H. Share, R. J. Murphy, R. A. Schwartz, A. Y. Shih, and R. P. Lin, High-resolution spectroscopy of gamma-ray lines from the x-class solar flare of 2002 July 23, *Astrophys. J., 595* , L81-L84, 2003.

Smith, D. M., A. Y. Shih, R. J. Murphy, G. H. Share, R. A. Schwartz, and R. P. Lin, *RHESSI* spectroscopy of nuclear de-excitation lines in x-class flares (abstract), *AAS Mtg. 204*, 02.01, 2004.

Tatischeff, V., J. Kiener, and M. Gros, Phyical implications of *INTEGRAL*/SPI gamma-ray line measurements of the 2003 October 28 solar flare, *Astron. Astrophys., 00*, 44-44, 2005

Toner, M. P., and A. L. MacKinnon,Do fast protons and α particles have the same energy distributions in solar flares?, *Solar Physics 223*, 155-168, 2004

Tylka, A. J., C. M. S. Cohen, W. F. Dietrich, S. Krucker, R. E. McGuire, R. A. Mewaldt, C. K. Ng, D. V. Reames, and G. H. Share, Onsets and release times in solar particle events, *Proc. of the 28th Cosmic Ray Conference, 7,* 3305-3308, 2003.

Tylka, A. J., C. M. S. Cohen, W. F. Dietrich, M. A. Lee, C. G. Maclennan, R. A. Mewaldt, C. K. Ng, and D. V. Reames, Shock geometry, seed populations, and the origin of variable elemental composition at high energies in large gradual solar particle events, *Astrophys. J.,* , 00-05, 2005.

G.H. Share and R.J. Murphy, E.O. Hulburt Center for Space Research Naval Research Laboratory Washington, DC 20375. (e-mail: gerald.share@nrl.navy.mil murphy@ssd5.nrl.navy.mil

Received ____________________

Figure 1. Cartoon showing particle acceleration, magnetic loop transport, interaction in the solar atmosphere, and interaction products. *Yohkoh* image of limb flare is shown in upper left corner (Masuda et al. 1994).

Figure 2. Fitted RHESSI count spectrum accumulated over the first 4 minutes of its observation of the 2003 Oct. 28 flare. Fits to the bremsstrahlung (dots), annihilation radiation (dots), α-^{4}He (dot-dot-dash), and narrow (solid), broad (dashes) and 2.22 MeV (dashes-dots) nuclear line components are shown separately.

Figure 3. Temporal variation of the bremsstrahlung power-law indices below (open diamonds) and above (filled diamonds) the break energy during the 2003 October 28 flare.

Figure 4. Temporal variation of the bremsstrahlung power-law index during the 1989 March 6 flare.

Figure 5. Fits to 4 lines observed during the 2003 October 28 flare. Top panels: ^{56}Fe and ^{24}Mg low FIP lines; Bottom panels: ^{12}C and ^{16}O high FIP lines. Dotted lines show the rest energies of the de-excitation lines.

Figure 6. Measurements of the % line shifts relative to the 4.43 MeV ^{12}C line vs. heliocentric angle made by SMM (squares) and RHESSI (solid circles, 2002 July 23: 72; 2003 Oct. 28: 30; Nov. 2: 60).

Figure 7. Fit to the integrated spectrum from the 2005 January 20 flare showing individual components.

Figure 8. Fit to *RHESSI* 2003 October 28 spectrum revealing the α-^{4}He contribution (dots) to the total spectrum after bremsstrahlung and other nuclear contributions have been removed; fits to the annihilation line (dashes) and continuum (solid curve) are also plotted. From share et al. 2004; reproduced courtesy of the Univ. of Chicago Press.

Figure 9. Broad nuclear-line component observed in the summed spectrum of 19 flares observed by *SMM.* The curve shows the calculated shape for accelerated particles with impulsive composition, α/p = 0.5, power-law index 4.5. The histogram is discussed in the text.

Figure 10. Broad ^{56}Fe/^{12}C line flux ratio in 19 *SMM* flares.

Figure 11. Nuclear to bremsstrahlung ratios vs. time observed by Yohkoh in the 2001 August 25 (top panel) and April 15 flares (middle panel) and by SMM in the 1989 March 6 flare (bottom panel).

Figure 12. Variation in Low FIP/High FIP line ratio observed in the 1989 March 6 flare observed by *SMM.*

Figure 13. Variation in Low FIP/High FIP line ratio observed in the 2003 October 28 and November 2 flares observed by *RHESSI.*

Figure 14. Time histories of the bremsstrahlung and total nuclear de-excitation line fluxes for the October 28 flare are plotted in the top two panels. Also shown are the time histories of the 511-keV annihilation line flux and width. From Share et al. (2004); reproduced courtesy of the Univ. of Chicago Press.

Figure 15. Count spectra of the solar 511-keV annihilation line (instrumentally broadened) derived by subtracting bremsstrahlung and nuclear contributions during the October 28 flare when the solar line was broad (11:06 - 11:16 UT) and narrow (11:18 - 11:30 UT). The solid curve is the best-fitting model that includes a Gaussian line and positronium continuum. From Share et al. (2004); reproduced courtesy of the Univ. of Chicago Press.

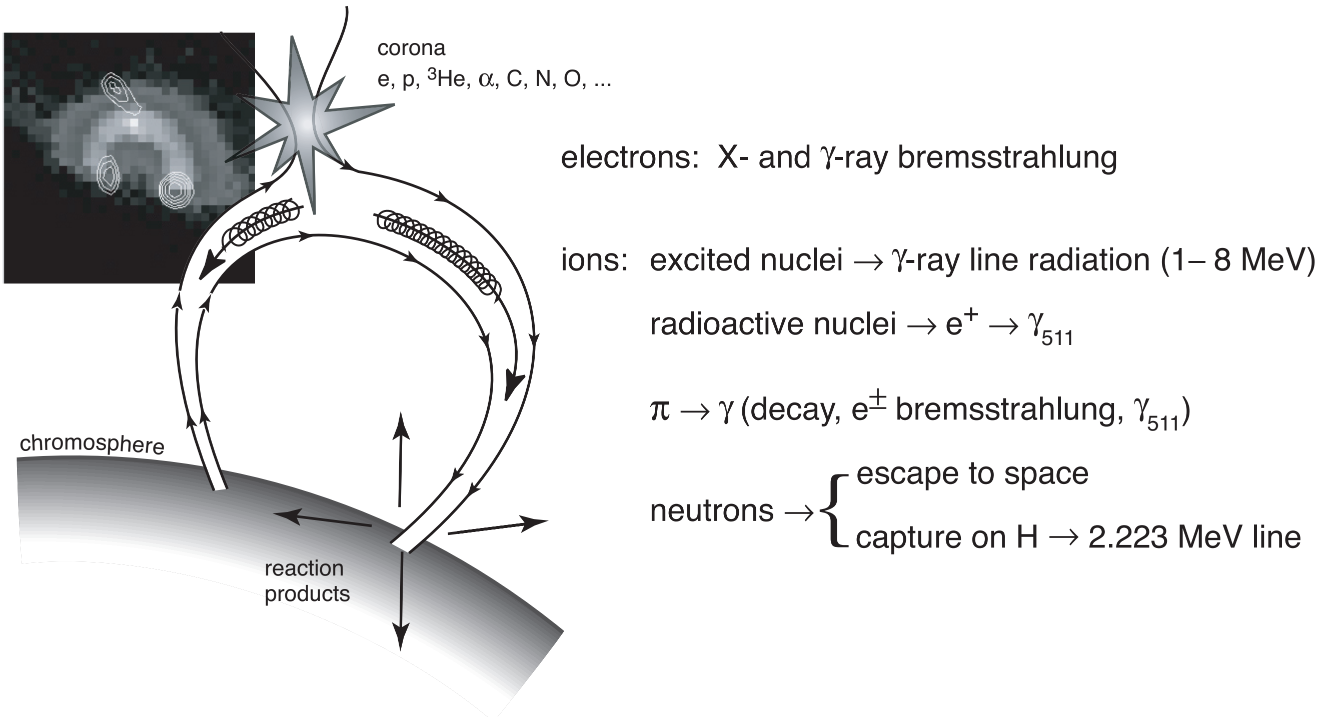
corona
e, p, ^{3}He, α, C, N, O, ...
electrons: X- and γ-ray bremsstrahlung
ions: excited nuclei $\rightarrow$ γ-ray line radiation (1– 8 MeV)
radioactive nuclei $\rightarrow e^+ \rightarrow \gamma_{511}$
$\pi \rightarrow \gamma$ (decay, $e^\pm$ bremsstrahlung, γ_{511})
neutrons $\rightarrow$ escape to space
capture on H $\rightarrow$ 2.223 MeV line
chromosphere
reaction products

Figure 1

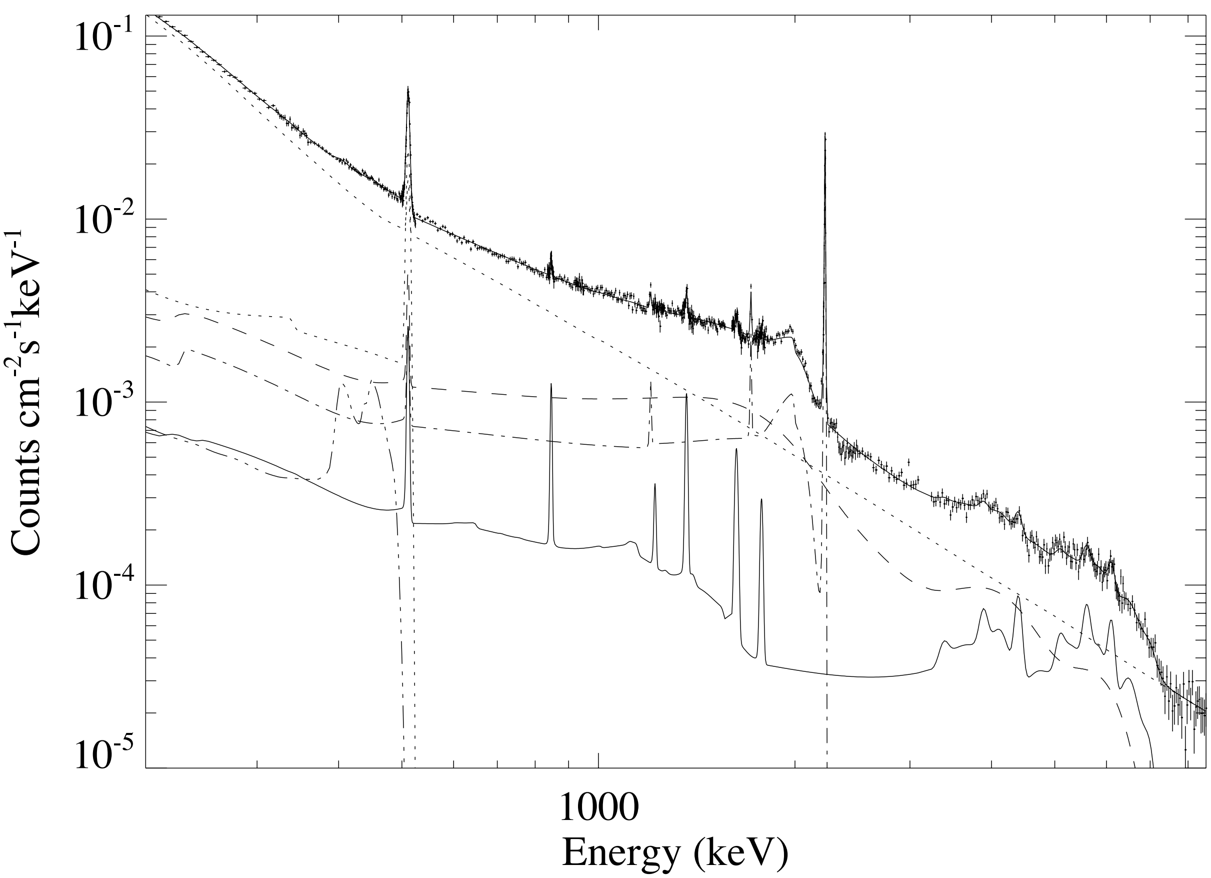

Figure 2

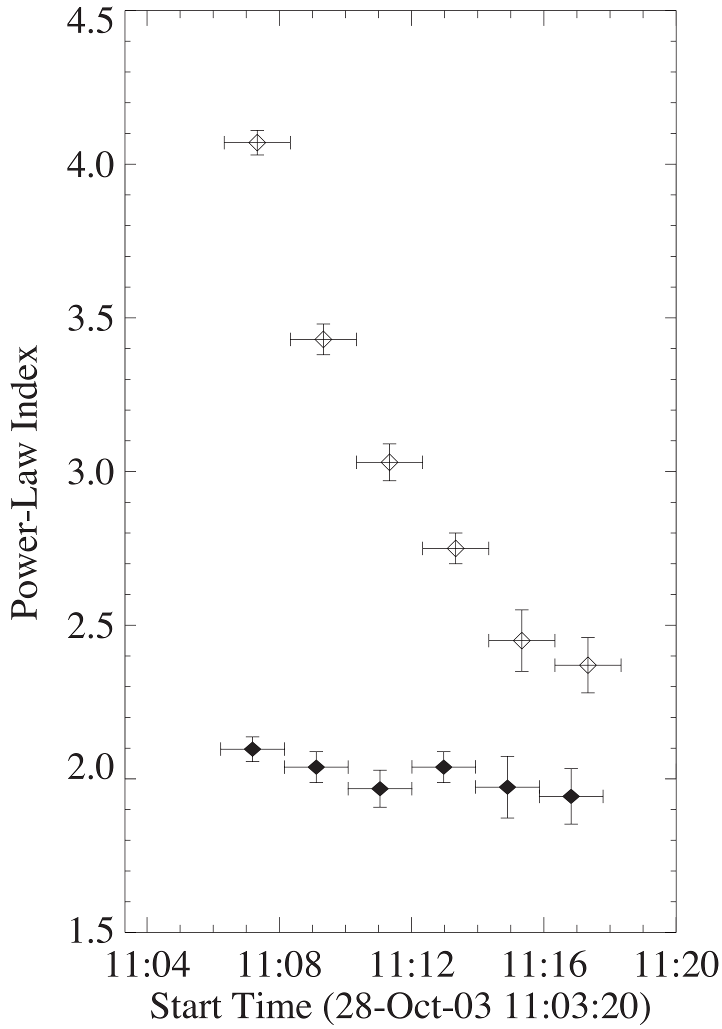

4.5
4.0
3.5
3.0
2.5
2.0
1.5
Power-Law Index
11:04
11:08
11:12
11:16
11:20
Start Time (28-Oct-03 11:03:20)

Figure 3

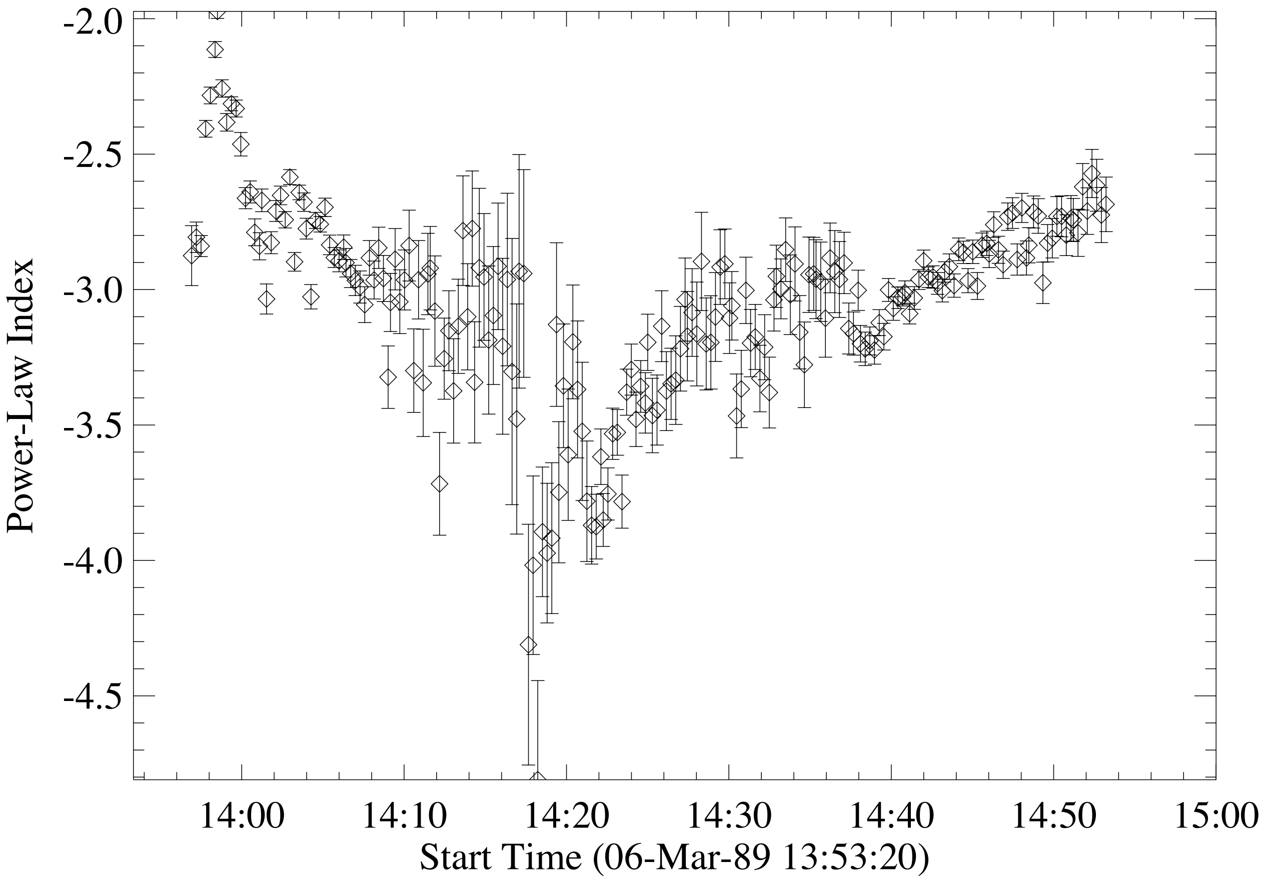

-2.0
-2.5
-3.0
-3.5
-4.0
-4.5
Power-Law Index
14:00
14:10
14:20
14:30
14:40
14:50
15:00
Start Time (06-Mar-89 13:53:20)

Figure 4

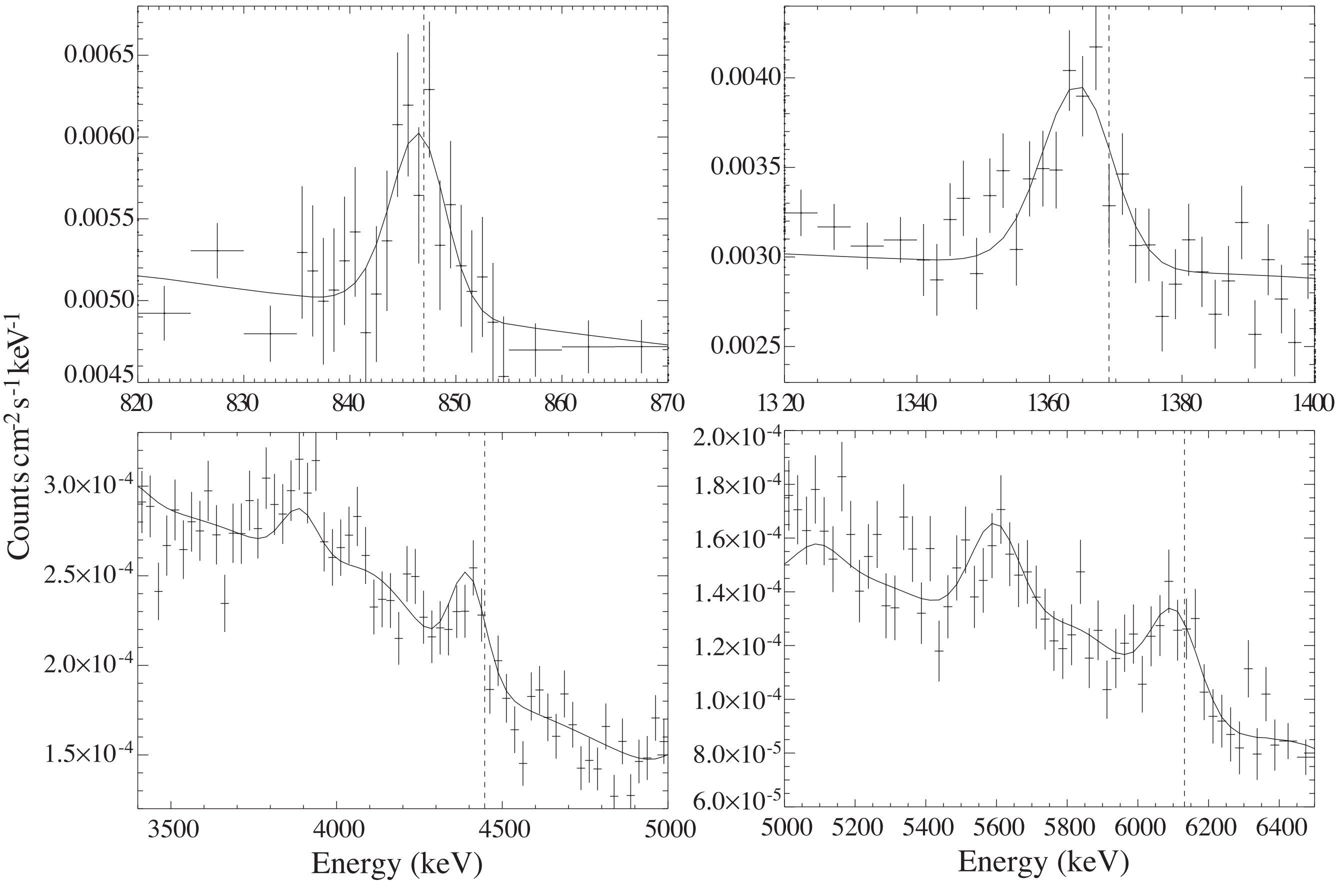

0.0065
0.0060
0.0055
0.0050
0.0045
820
830
840
850
860
870
0.0040
0.0035
0.0030
0.0025
1320
1340
1360
1380
1400
Counts cm-2 s-1 keV-1
3.0×10-4
2.5×10-4
2.0×10-4
1.5×10-4
3500
4000
4500
5000
Energy (keV)
2.0×10-4
1.8×10-4
1.6×10-4
1.4×10-4
1.2×10-4
1.0×10-4
8.0×10-5
6.0×10-5
5000
5200
5400
5600
5800
6000
6200
6400
Energy (keV)

Figure 5

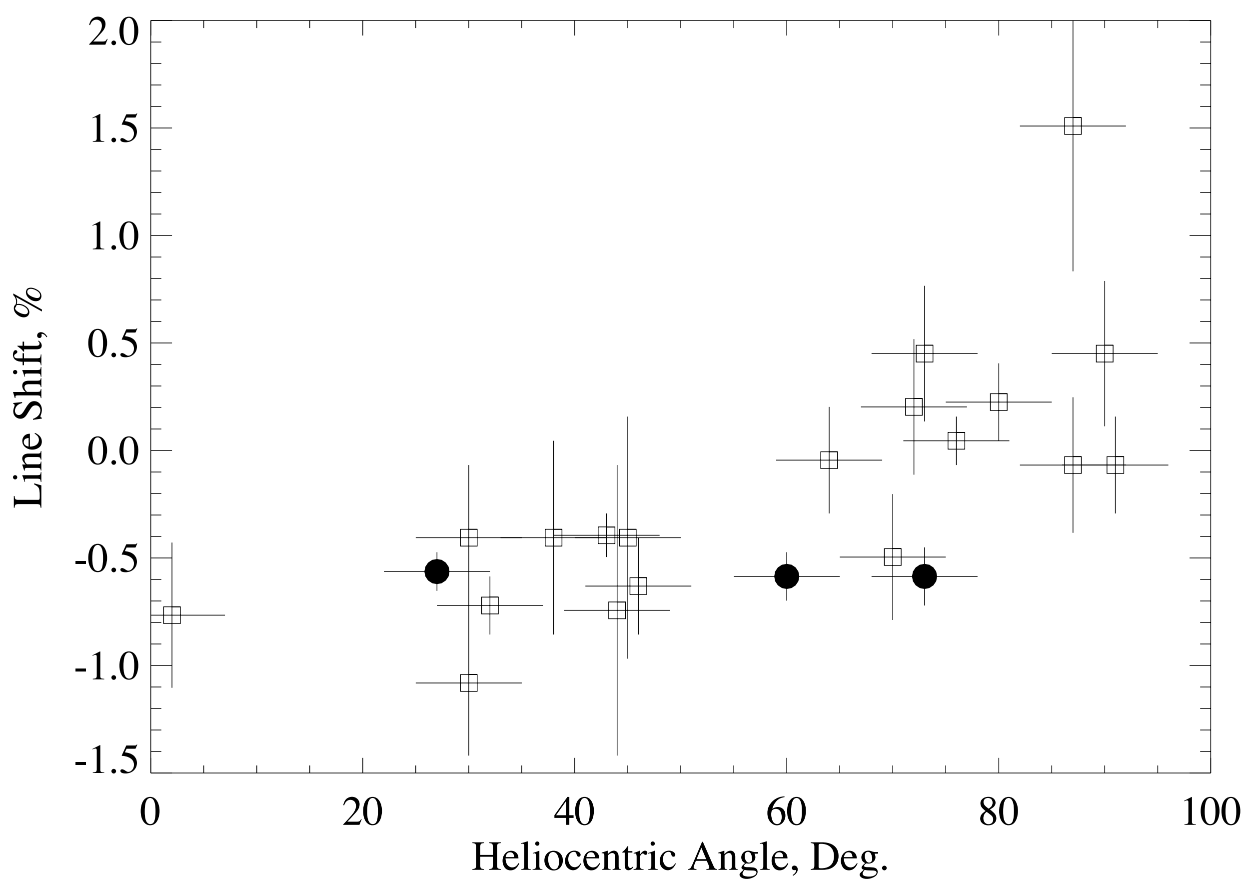

2.0
1.5
1.0
0.5
0.0
-0.5
-1.0
-1.5
Line Shift, %
0
20
40
60
80
100
Heliocentric Angle, Deg.

Figure 6

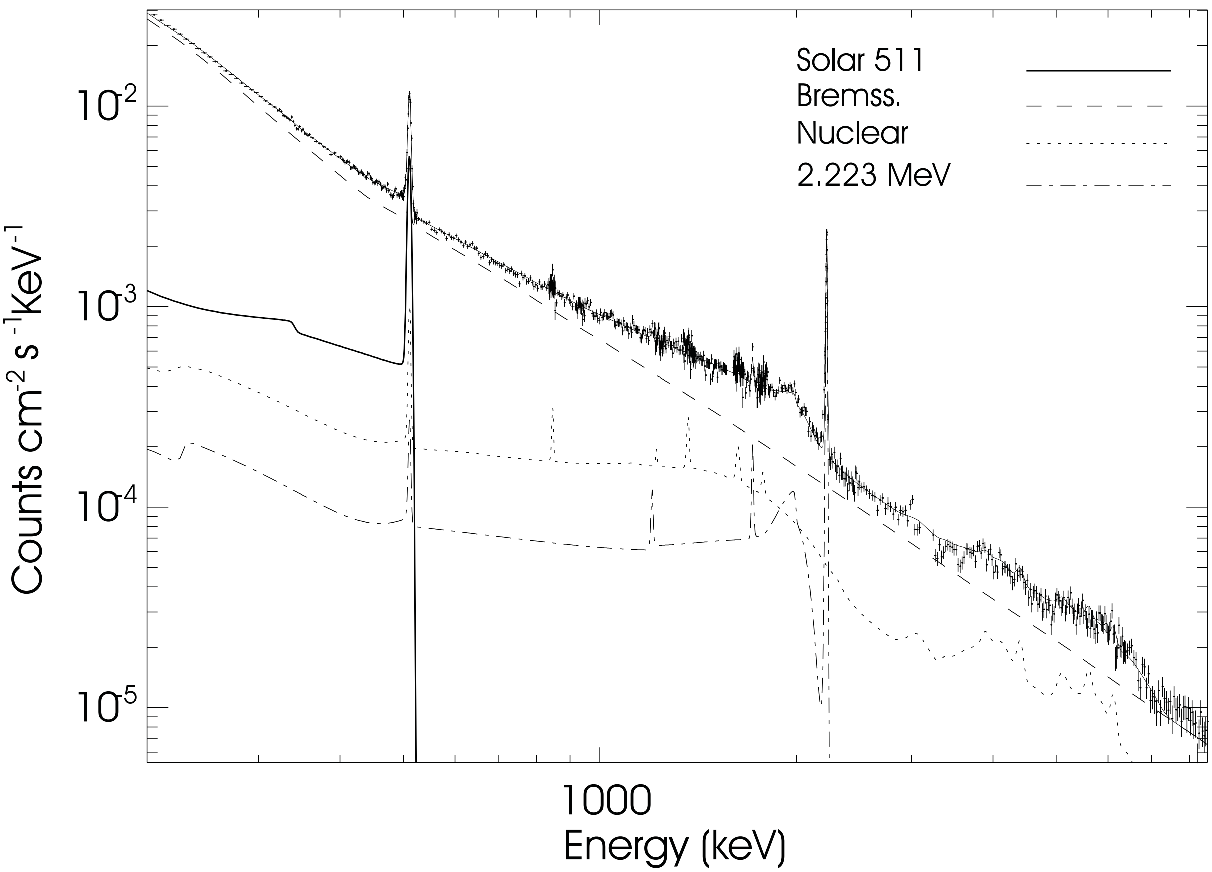

Solar 511
Bremss.
Nuclear
2.223 MeV
10^{-2}
10^{-3}
10^{-4}
10^{-5}
Counts cm^{-2} s^{-1}keV^{-1}
1000
Energy (keV)

Figure 7

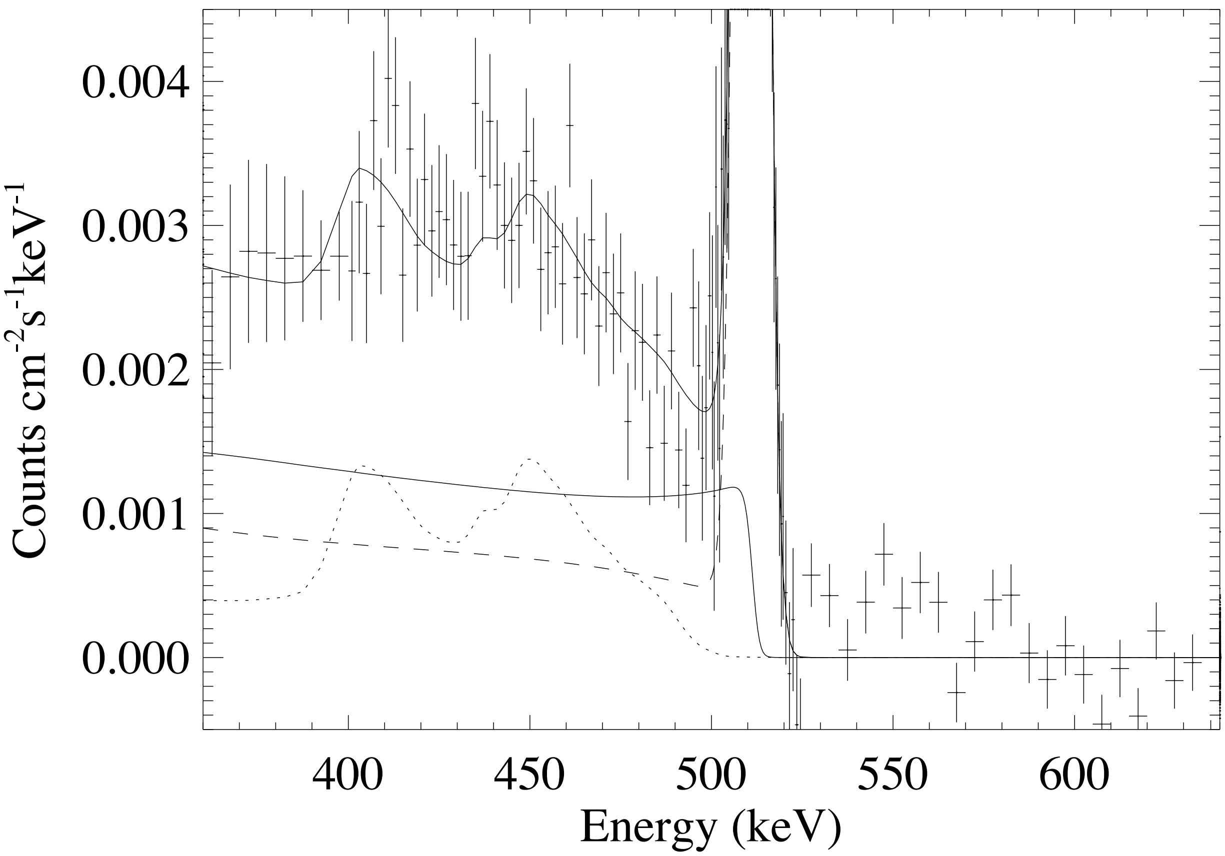
0.004
0.003
0.002
0.001
0.000
Counts cm^{-2}s^{-1}keV^{-1}
400
450
500
550
600
Energy (keV)

Figure 8

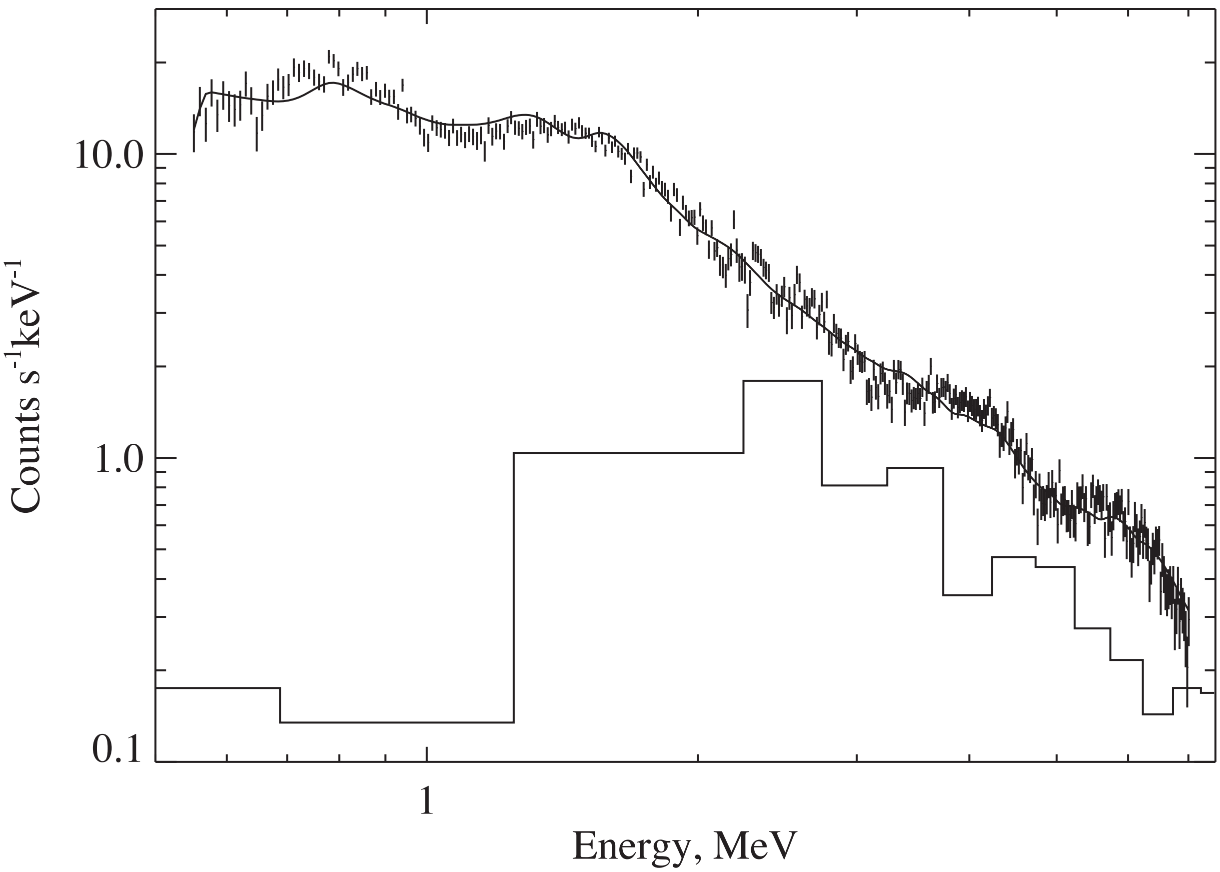

Figure 9

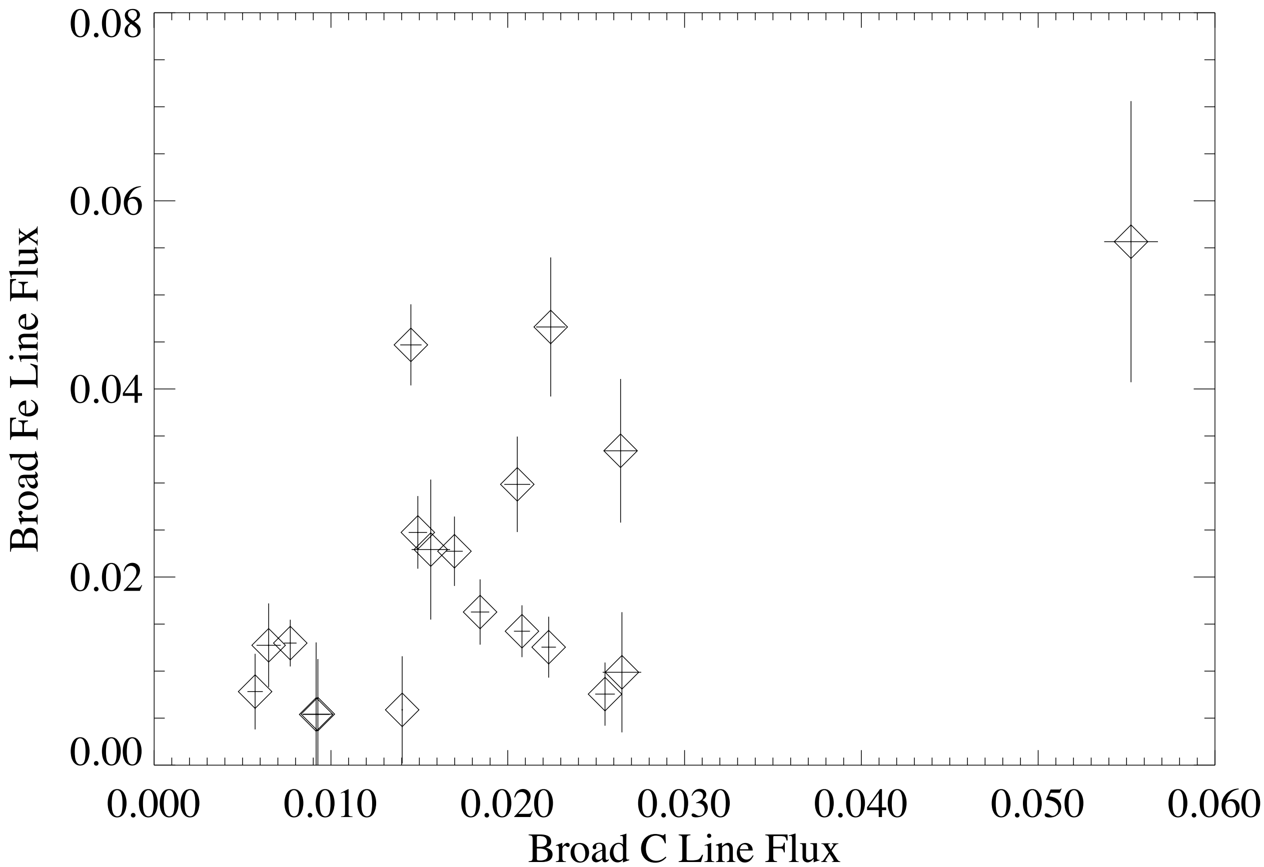
0.08
0.06
0.04
0.02
0.00
Broad Fe Line Flux
0.000
0.010
0.020
0.030
0.040
0.050
0.060
Broad C Line Flux

Figure 10

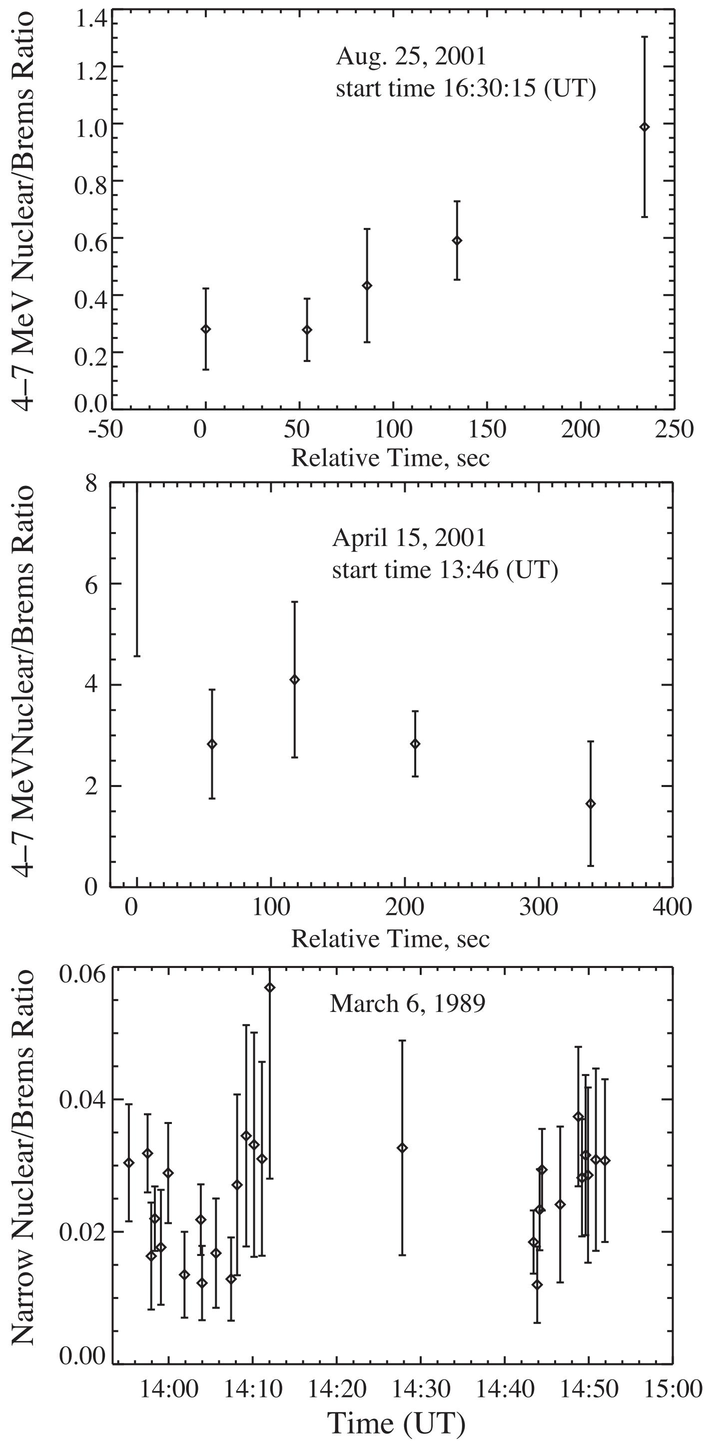

Aug. 25, 2001
start time 16:30:15 (UT)
4–7 MeV Nuclear/Brems Ratio
Relative Time, sec
April 15, 2001
start time 13:46 (UT)
4–7 MeVNuclear/Brems Ratio
Relative Time, sec
March 6, 1989
Narrow Nuclear/Brems Ratio
Time (UT)

Figure 11

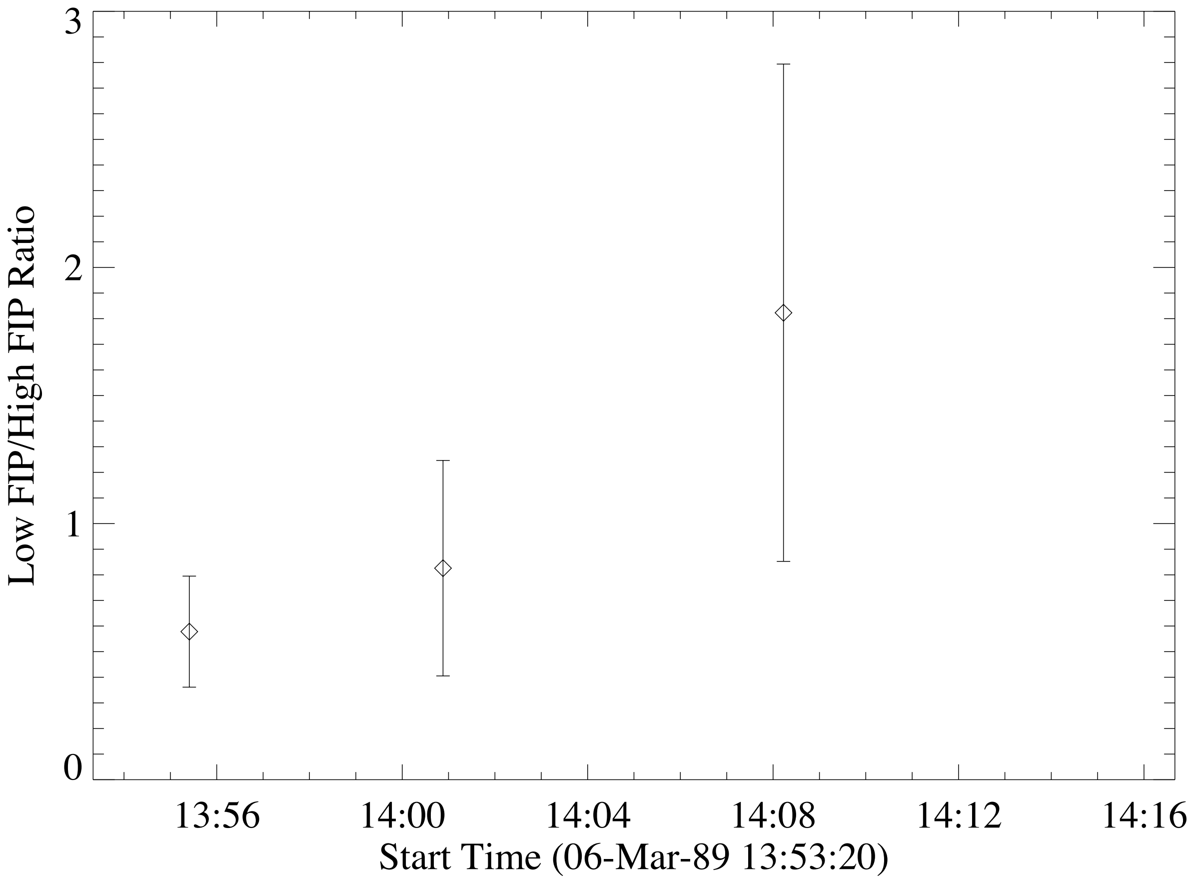
3
2
1
0
Low FIP/High FIP Ratio
13:56
14:00
14:04
14:08
14:12
14:16
Start Time (06-Mar-89 13:53:20)

Figure 12

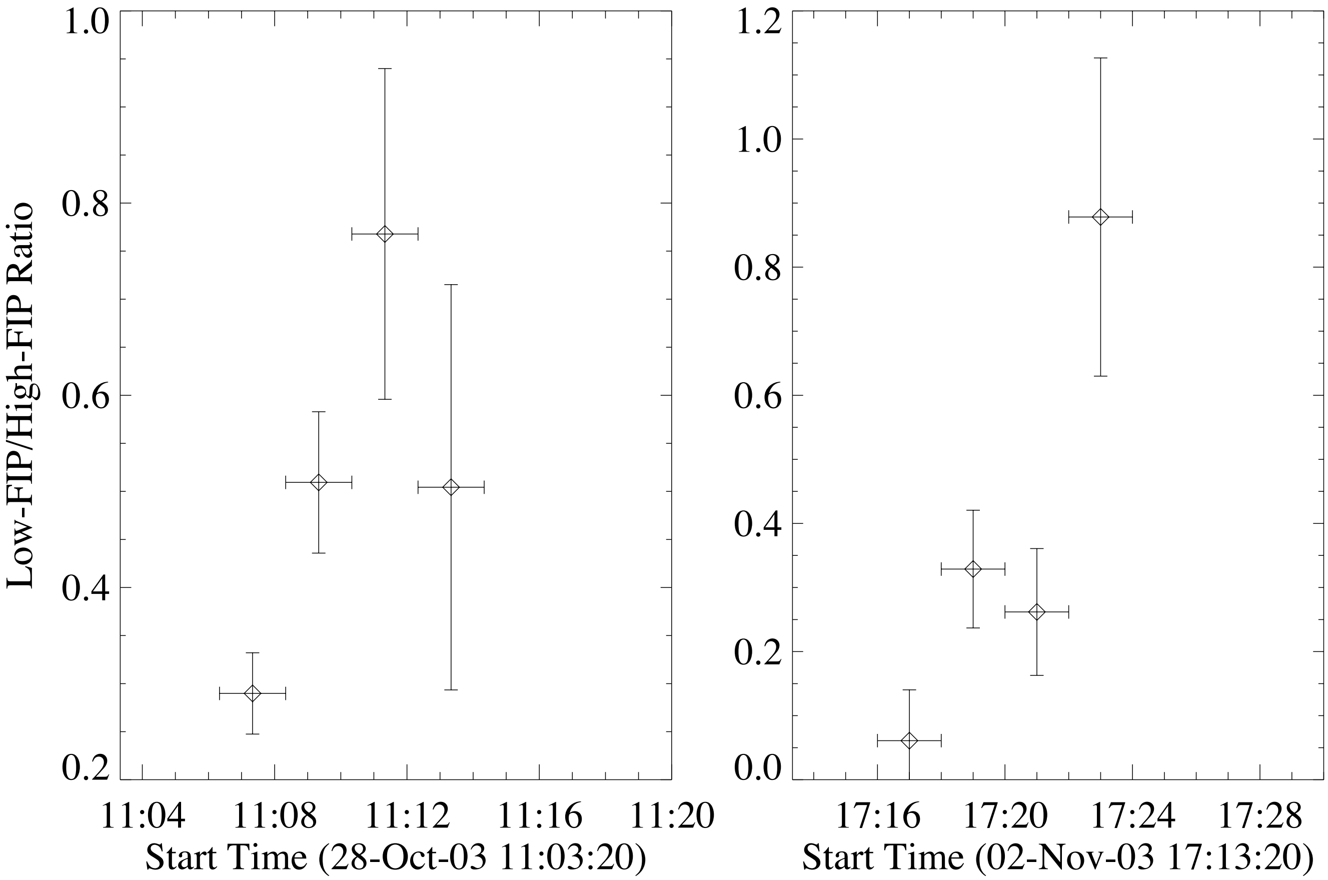

Low-FIP/High-FIP Ratio
1.0
0.8
0.6
0.4
0.2
11:04
11:08
11:12
11:16
11:20
Start Time (28-Oct-03 11:03:20)
1.2
1.0
0.8
0.6
0.4
0.2
0.0
17:16
17:20
17:24
17:28
Start Time (02-Nov-03 17:13:20)

Figure 13

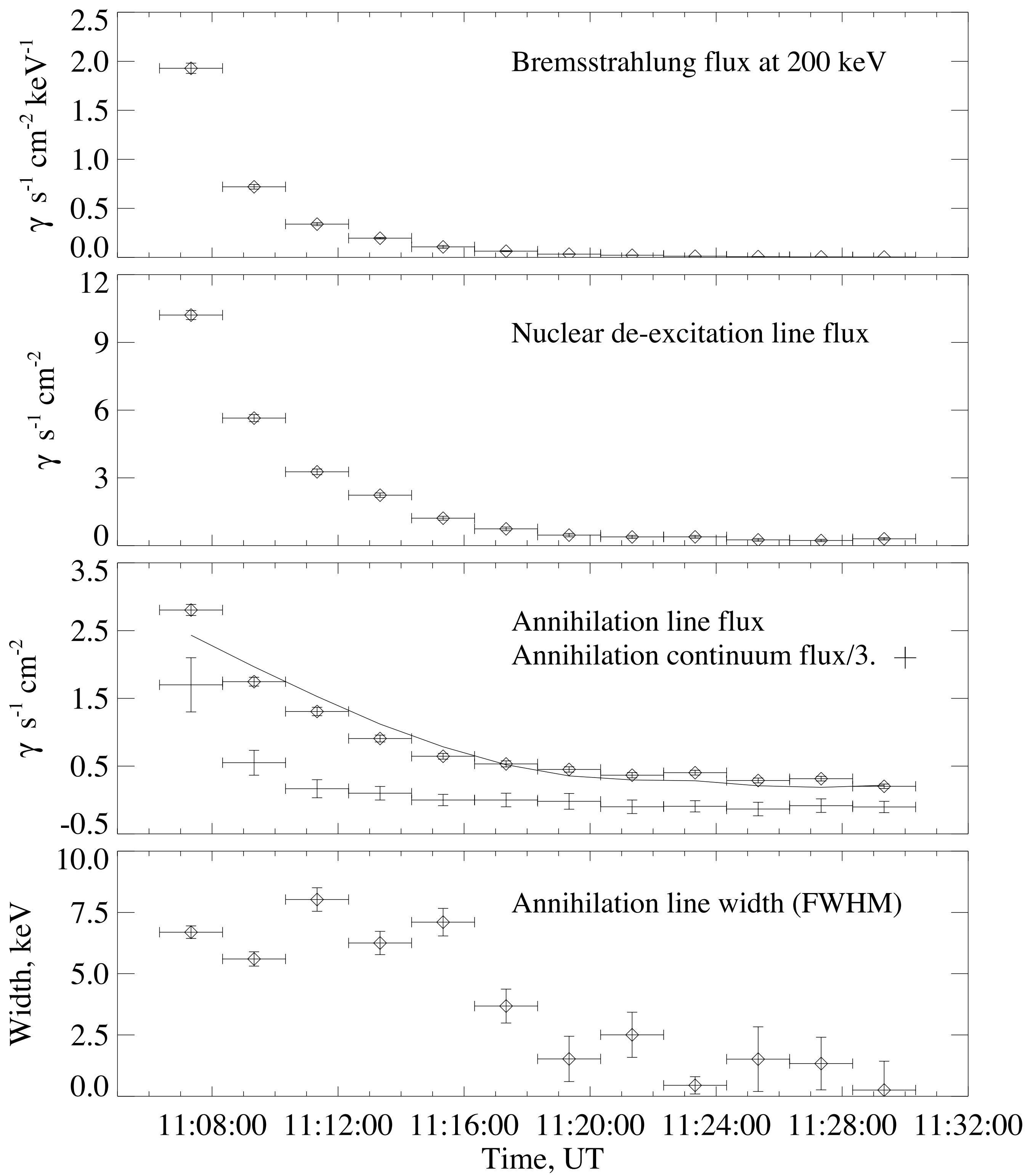

Bremsstrahlung flux at 200 keV
γ s-1 cm-2 keV-1
Nuclear de-excitation line flux
γ s-1 cm-2
Annihilation line flux
Annihilation continuum flux/3.
γ s-1 cm-2
Annihilation line width (FWHM)
Width, keV
11:08:00
11:12:00
11:16:00
11:20:00
11:24:00
11:28:00
11:32:00
Time, UT

Figure 14

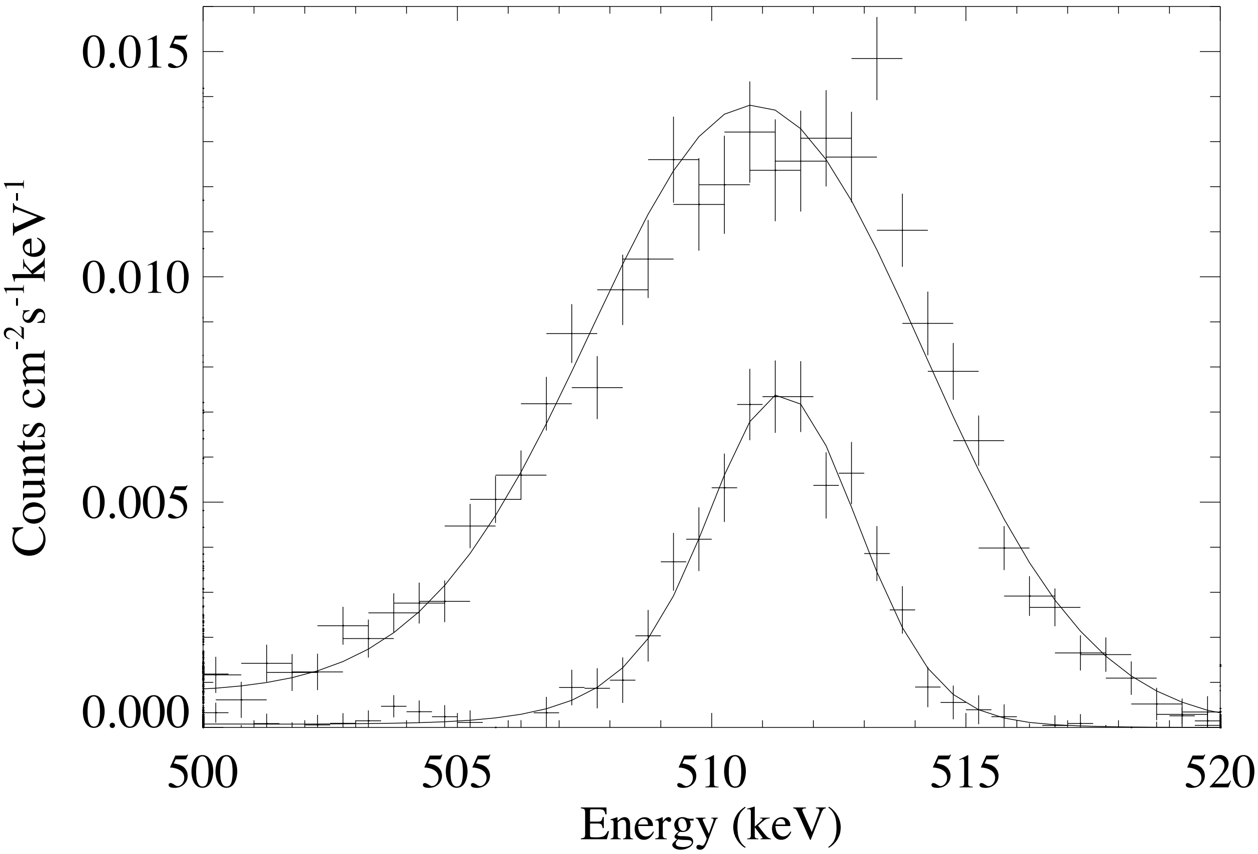
0.015
0.010
0.005
0.000
Counts cm^{-2}s^{-1}keV^{-1}
500
505
510
515
520
Energy (keV)

Figure 15